

Journal of Materials Chemistry A

Accepted Manuscript



This is an *Accepted Manuscript*, which has been through the Royal Society of Chemistry peer review process and has been accepted for publication.

Accepted Manuscripts are published online shortly after acceptance, before technical editing, formatting and proof reading. Using this free service, authors can make their results available to the community, in citable form, before we publish the edited article. We will replace this *Accepted Manuscript* with the edited and formatted *Advance Article* as soon as it is available.

You can find more information about *Accepted Manuscripts* in the [Information for Authors](#).

Please note that technical editing may introduce minor changes to the text and/or graphics, which may alter content. The journal's standard [Terms & Conditions](#) and the [Ethical guidelines](#) still apply. In no event shall the Royal Society of Chemistry be held responsible for any errors or omissions in this *Accepted Manuscript* or any consequences arising from the use of any information it contains.

Polyoxometalate Coupled Graphene Oxide-Nafion Composite Membrane for Fuel Cell Operating at Low Relative Humidity

Yong Kim^a, Kriangsak Ketpang^a, Shayapat Jaritphun^b, Jun-Seo Park^b, and Sangaraju Shanmugam^{a,*}

^a Department of Energy Systems Engineering, Daegu Gyeongbuk Institute of Science and Technology (DGIST), 50-1 Sang-Ri, Hyeonpung-Myeon, Dalseong-Gun, Daegu 711-873, Republic of Korea

^b Department of Chemical Engineering and Research Centre of Chemical Technology, Hankyong National University, Anseong, Gyeonggi 456-749, Republic of Korea

E-mail: sangarajus@dgist.ac.kr

Abstract

Polymer electrolyte fuel cells operated at elevated temperature and low relative humidity (RH) have been investigated by utilizing polyoxometalate coupled with graphene oxide-Nafion membrane. Phosphotungstic acid (PW) coupled graphene oxide-Nafion (Nafion/PW-mGO) membrane showed enhanced proton conductivity compared with pristine and recast Nafion membranes. Nafion/PW-mGO hybrid membrane exhibited a maximum power density of 841 mW cm⁻², whereas pristine Nafion membrane showed a power density of 210 mW cm⁻² at 100 % RH. In addition, our hybrid membrane showed a 4-fold higher maximum fuel cell power density operated at 80°C under 20% RH, compared with a state-of-the-art pristine membrane (Nafion-212). The remarkable enhanced performance of Nafion/PW-mGO composite membrane was mainly attributed to the reduction of ohmic resistance by the hygroscopic solid acids, which can retain water in their framework through the hydrogen bonding with protons at elevated temperatures and facilitates proton transport through the membrane.

Introduction

Polymer electrolyte fuel cells (PEFC) are attracting tremendous interest as one of the most promising clean power generation techniques to alter the use of fossil energy sources.¹ Researchers have paid great efforts to develop the fuel cell for commercialization based on hydrogen energy to reduce the amount of oil being used and to decrease emission of global warming pollutants.¹ However, a profound drawback of current PEFC technology utilizes Nafion, which has low water retention at temperatures above 80 °C or inability to operate under low humidity for extended periods.²⁻⁶ The proton conductivity of Nafion membrane is very sensitive to water content and is maximal when fully saturated with water.^{7,8} Retention of water within the membrane at and above 80 °C is a key parameter to achieve high proton conductivity of Nafion based membranes. At elevated temperature and low relative humidity (RH) the proton of Nafion membrane conductivity decreases dramatically by orders of magnitude due to the membrane dehydration, thus the operation of PEFCs at low RH is limited, so the current Nafion and other membranes can not meet the requirements for the practical applications of PEFC and impede commercialization of this technology.^{9,10}

Several approaches were adopted to alter and improve the physical and chemical properties of Nafion membrane. One promising approach to enhance the performance of membranes is to increase the ion-exchange capacity (IEC) by adding ionic groups to the polymer, resulting in increasing the proton conductivity. However, the membrane with high IEC value exhibits a poor mechanical property due to its excessive swelling behavior. Yet another approach to improve the proton conductivity of Nafion membranes at low humidity is to include inorganic fillers such as silica,¹¹⁻¹³ titania,¹³⁻¹⁵ zirconia,¹⁶ clay¹⁷ etc., which authorize both hygroscopic and proton conductive properties in the membrane. Hygroscopic inorganic fillers narrows the hydrophilic channels and retains water in the Nafion matrix, facilitating the proton conduction.^{11,12,16} Another aspect of inorganic fillers, exhibit high

thermal stability over 100 °C owing to the electrostatic attraction within the electrical double layer.¹⁵ Nevertheless, incorporating inorganic materials in Nafion reduce the proton conductivity owing to a decrease in the number of sulfonate groups per unit volume of each domain.¹³

Polyoxometalates (POM) are well defined metal-oxygen cluster compounds, received much attention in recent years due to their high acid strength and thermal stability.^{18,19} The protons present in POM form hydrogen bonds with water in the crystal structure and exist as H_3O^+ or H_5O_2^+ , so it is a prospective material in the field of proton exchange fuel cell for high proton conductive membrane with Nafion.¹⁹⁻²² Nafion/polyoxometalate composite membrane can improve proton conductivity, but embedded polyoxometalate can be leached out from the membrane due to its high solubility in water.²² As this problem remains, new approaches are needed. To address this serious issue, one of the promising approaches is the construction of nanostructured hybrid, in which ionic clusters are coupled with graphene oxide surface with a linker forming strong electrostatic coupling between POM and GO materials.

Herein, we introduce a rational design of nanohybrid consisting of phosphotungstic acid, $\text{H}_3[\text{PW}_{12}\text{O}_{40}]\cdot 29\text{H}_2\text{O}$ (PW) coupled with a covalent modification of reduced graphene oxide with a 3-aminopropyl-triethoxysilane (APTES), through an electrostatic interaction between the (PW) and the graphene oxide surface via a silane linker, amine group (mGO). The linker, APTES is a strong base, so that it makes a strong electrostatic interaction with PW caused by brönsted acid and brönsted base states. Further, the silane group attaches with the hydroxyl group and the carboxyl group on the reduced graphene oxide (rGO) through condensation reaction as depicted in Fig. 1.

Results and discussion

The formation of PW-mGO nanohybrid was first characterized by FT-IR, TEM and CV techniques. The FT-IR spectra of GO, rGO, mGO, and PW-mGO showed characteristic individual functional group vibration peaks as shown in Fig. 2a. The successful hybridization of the APTES onto the reduced graphene oxide was confirmed by its characteristic stretching peaks of -NH_2 and Si-O in a range of 2000 to 700 cm^{-1} .²³ The absorption peaks at 3275 cm^{-1} , 1574 cm^{-1} , and 774 cm^{-1} attributed to the -NH_2 functional group.²³ The Si-O-C peak (1045 cm^{-1}) and Si-O-Si peak (1119 cm^{-1}), overlapped and giving rise a broad peak, indicating the successful hybridization of APTES onto the reduced graphene oxide through the condensation reaction. The FT-IR spectra of pure PW displayed four M-O characteristic stretching peaks at 1080 (P-O), 983 (W=O_t), 891($\text{W-O}_b\text{-W}$) and 803 cm^{-1} ($\text{W-O}_c\text{-W}$). Compared with pure PW, peaks of the hybrid composite, PW-mGO (Fig. 2b) at 1036 (P-O), 972 (W=O_t), 884 ($\text{W-O}_b\text{-W}$) and 806 cm^{-1} ($\text{W-O}_c\text{-W}$) indicated red shift, that may be ascribed to the strong interaction between amine group on the modified graphene oxide and PW due to strong adsorption via electrostatic binding between them. The TEM morphology analysis of PW-mGO hybrid reveals that the PW clusters dispersed uniformly with a cluster size of 1-2 nm on the graphene sheet (Fig.3a). The well dispersed state of individual PW clusters suggests that the PW strongly attached to the carbon framework of graphene. Moreover, TEM-HAADF images further shows the size of PW clusters were in the range of 1-2 nm (Fig. 3b,c). The loading of PW coupled on the surface of mGO was determined by thermogravimetric analysis (Fig. S1). The thermograms showed GO was completely decomposed at 700 °C. Based on thermogravimetric analysis of mGO and PW-mGO, the contents of APTES and PW in mGO and PW-mGO was found to be 9 and 15 wt%, respectively.

Figure 4a shows the cyclic voltammograms (CV) of pure PW and PW-mGO hybrid electrodes in a potential window of -0.75 to -0.25 V at a scan rate of 25 mVs⁻¹. The anodic and cathodic peak potentials and peak separation was listed in Table 1. A significant peak shift to more negative potential was observed for PW-mGO electrode when compared with pure PW. The observed negative peak shift might be due to PW energy levels stabilization, which is due to a strong interaction with the graphene oxide surface can be expected. This phenomenon was seen as same reason from FT-IR data, which described a red shift caused by coating APTES on the rGO surface. Figure 4b presents the CVs of PW-mGO at different scan rates (from 10 to 500 mVs⁻¹). The anodic and cathodic peak currents increased with the increasing the scan rate. The peak separation potential values were gradually increased with increasing scan rate, indicated that the electrochemical redox process is surface dominate electron transfer phenomenon. Generally, the POM modified electrode films are usually unstable when applied in aqueous media during the electrochemical studies, which is due to their high solubility in aqueous solution, resulting in a decay of current. So, we evaluate the electrochemical stability of the PW-mGO hybrid electrode in 1M H₂SO₄, by continuous CV cycling stability test was performed with a scan rate of 50 mV s⁻¹ for 200 cycles (Fig. S2a). The decay of the first reduction peak current was found to only 4.5%, indicating a good electrochemical stability of the PW-mGO hybrid, which is due to the strong coupling between the amino group of APTES and PW (Fig. S2b).

After successful fabrication of PW-mGO nanohybrid, the PW-mGO is incorporated in the Nafion ionomer and cast the composite membrane. The optimum PW-mGO nanohybrid loading in the composite membrane was found to be 1 wt% to the Nafion ionomer based on the proton conductivity and fuel cell performance studies (Fig. S3a, b). The composite membranes were further evaluated the fuel cell performance and compared with that of recast Nafion and Nafion-212 membranes. The catalyst loading on gas diffusion layers was kept

identical for all the MEA studies. Figure 5a compares the polarization plots of recast Nafion, Nafion-212, Nafion/mGO and Nafion/PW-mGO composite membranes at 80 °C under ~100% RH and ambient pressure. The open circuit voltage was roughly 0.99 -1.03 V for all membranes, indicating very small amount of H₂ gas permeability from the anode to the cathode through the membrane (Fig. 5). Nafion/mGO, Nafion/PW-mGO composite membranes delivered a maximum power density of 537, and 826 mW cm⁻², respectively. The Nafion-212 and recast Nafion membranes delivered maximum power density of 599 and 598 mW cm⁻², respectively. The power density of Nafion/PW-mGO was 1.38 folds higher than Nafion-212 membrane (Fig. 5a). Furthermore, the Nafion/PW-mGO composite membrane also provided higher current density than the Nafion-212 and recast Nafion membranes. Generally, it is known that the fuel cell performance is closely related to the issue of water management. Nafion/mGO membrane limited availability of water at the anode, electro-osmotic drag of water from the anode to the cathode and insufficient water back-diffusion from the cathode to the anode causes the MEA to dehydrate owing to not smooth and homogeneous state of membranes.

The fuel cell performance was further evaluated at 80 °C under 20 %RH for all membranes (Fig. 5b). The Nafion/mGO and Nafion/PW-mGO composite membranes exhibited the maximum power density of 488, and 841 mWcm⁻², respectively. The Nafion-212 and recast Nafion membranes delivered maximum power density of 210 and 208 mWcm⁻², respectively. The maximum power density of Nafion/mGO and Nafion/PW-mGO membranes was approximately 2.3- and 4.0-folds higher than pristine Nafion-212 membrane, respectively (Table 2). The results of fuel cell performance of Nafion/mGO and Nafion/PW-mGO composite membranes clearly showed an improved performance at low humidity, especially, Nafion/PW-mGO composite membrane exhibited a remarkable enhancement of the fuel cell performance operated at low RH compared to Nafion-212 and

recast Nafion membranes. Even though, Nafion/mGO composite membrane showed lower maximum power density at fully RH condition, but they exhibited improved current density and power density under low humidity fuel cell operation. This can be attributed to the presence of oxygen functional groups, such as hydroxyl, carboxylic on GO surface, which can be easily hydrated.²⁴⁻²⁷ These acidic functional groups and intermolecular hydrogen bonding can provide more proton conduction pathways in addition to Nafion sulfonic acid groups.²⁴⁻²⁷ It is obvious that Nafion/PW-mGO and Nafion-mGO exhibits substantially lower ohmic resistance than Nafion-212 and recast Nafion membranes (Table 2). The superior fuel cell performance could be exclusively attributed to the Nafion/PW-mGO composite membrane, as the electrodes (anode, cathode) composition and preparation kept identical for all membrane electrode assemblies. The maximum power density at low humidity operating fuel cell of our Nafion/PW-mGO membrane was compared with various Nafion composite membranes as listed in Table 3.²⁸⁻³⁵ The Nafion/PW-mGO composite membrane exhibited remarkably higher maximum power density under low RH compared to Nafion/TiO₂ nanotube,¹⁵ Nafion/CsPMo,³² and Nafion/GO.³⁴ Eventually, our composite membrane, Nafion/PW-mGO, showed highest power density and to the best of the authors' knowledge, this is the highest maximum power density observed for Nafion composite membranes at low RH.

The fuel cell performance of composite membranes was evaluated and compared with recast Nafion and pristine Nafion-212 membranes under ~100% RH at 100 °C and under ambient conditions (Fig. S4). The Nafion-212 and Nafion/PW-mGO composite membranes provided the maximum power density of 489, and 616 mWcm⁻², respectively. The power density of Nafion/PW-mGO, Nafion/mGO composite membranes at 0.6 V was 591, 452 mW cm⁻², respectively. The Nafion-212 and recast Nafion membranes delivered power density values of 463 and 453 mW cm⁻², respectively, at the same potential. At 100 °C, the fuel cell

performance of the Nafion/PW-mGO composite membrane was substantially higher than the recast Nafion and Nafion-212 membranes under 100% RH. The current density of the composite membranes was also higher than Nafion-212 and recast Nafion membranes. Next we compared the practical power density at 0.6 V of the Nafion/PW-mGO membrane under cell operation temperature of 100 °C was ultimately 1.3 times higher than that of the Nafion-212 membrane. The higher PEFCs performance of Nafion/PW-mGO composite membrane was obviously due to the hygroscopic property and strong acid strength of PW cluster compounds, which can retain water at temperature greater than 100 °C.

To clarify the high performance of composite membrane toward Nafion-212 membrane, the proton conductivity for Nafion/mGO, Nafion/PW-mGO composite membranes was investigated in comparison the conductivity result obtained from Nafion-212 membrane. It has been demonstrated that the morphology of Nafion membrane composes of hydrophobic PTFE back bone and hydrophilic perfluoro sulfonic acid group (ionic cluster).^{5,8} The proton conductivity of Nafion membrane highly depends on the water content adsorbed in the membrane. At low water content (low RH), the proton conductivity is low because insufficient water is absorbed in the ionic cluster, resulting in lack of connectivity between ionic clusters. On the other hand, as more water is absorbed in the membrane (100% RH), the ionic cluster is expanded and eventually the expanded ionic clusters are connected each other, yielding greatly increase of proton conductivity.^{5,8} Figure 6 shows the proton conductivity of Nafion-212, Nafion/mGO, and Nafion/PW-mGO membranes at different RH conditions. The proton conductivity of Nafion-212 membrane under a 100% RH of humidified condition was 98 mS cm⁻¹ at 80 °C. The proton conductivity of the Nafion-212 membrane decreases as the RH value decreases; at 25% RH, the conductivity of the Nafion membrane was 6.5 mS cm⁻¹. However, Nafion/mGO composite membrane showed enhanced proton conductivity at all relative humidities and the proton conductivity under a 100% RH of humidified condition

was 117 mS cm^{-1} at 80°C , and at 25% RH, the conductivity of the Nafion/mGO membrane was 9.2 mS cm^{-1} , expected end functional group of graphene oxide, which adhered APTES containing amine group was attracted to water *via* hydrogen interaction. It has been reported that Nafion-graphene oxide composite membrane showed higher proton conductivity than pristine Nafion membrane owing to hydrogen bond with water led to functional group on the graphene oxide such as hydroxyl, carboxyl, and epoxy group.^{26,27} The modified graphene oxide was functioned similarly in the membrane that the high proton conductivity of the composite membrane is attributed to a Grotthus type mechanism, wherein reorganization of hydrogen bonds plays a vital role in hydrated graphene.^{26,27} The proton conductivity of the Nafion/PW-mGO composite membranes is the highest among these membranes at all RH values (Fig. 6). Under a fully humidified condition, maximum proton conductivity of 159 mS cm^{-1} , and at 25% RH, the conductivity of 10.4 mS cm^{-1} , is exhibited by the Nafion/PW-mGO composite membrane. The presences of phosphotungstic acid clusters provide more facile hopping of protons, thereby, increasing the proton transport. In other words, Nafion/PW-mGO composite membrane has enhanced water-holding capacity due to strong absorption of water on heteropolyanion clusters possesses hydronium ion, so that it serves to retain proton conductivity.³⁶ Generally, the polyoxometalates are capable of sustaining a large number of water molecules in their hydration sphere, and they behave like pseudo-liquids, so that the proton migration can be as effective as in aqueous electrolyte solutions.¹⁹ This effect is much influenced to the total hydration number at low hydration level of composite membrane. To verify the improved proton conductivity of Nafion/PW-mGO composite membrane, the water uptake and ion exchange capacity were estimated. Proton conductivity of the membrane depends to a large extent on the amount of water uptake and ion exchange capacity.³⁷ The water uptake of recast Nafion, Nafion/mGO, and Nafion/PW-mGO membranes was found to be 27, 32 and 37%, respectively. And the ion exchange capacity

(IEC) of recast Nafion, Nafion/mGO, and Nafion/PW-mGO membranes was 0.88, 0.88 and 0.84 mmol g⁻¹ at room temperature. The IEC of Nafion/PW-mGO composite membrane was found to be lower than Nafion membrane. The lower IEC value of composite membrane can be attributed to the obscuring the exchange of sodium ions during the titration, which could be due to the decrease of the number of ionic channels in composite membrane.

Fig.S5a presents the fuel cell durability studies of Nafion/PW-mGO and Nafion-212 membranes for 120 h under 18% RH at 80 °C. The OCV of the Nafion/PW-mGO and Nafion-212 membranes decreased from 1.03 to 0.95 V and 1.01 to 0.58 V, respectively. The Nafion/PW-mGO membrane showed a stabilized OCV within 10 h of operation, then thereafter the rate of OCV decrease is minimum. On the other hand, Nafion-212 membrane showed steep decrease in OCV and reached 0.5 V within a span of 120 h, indicating PW clusters are strongly anchored to the mGO surface, thus provide better conductivity and exhibits stable fuel cell performance.

The mechanical property of composite membrane was determined using tensile test and compared with recast Nafion membrane and results are shown in Fig. S5b. The Young's modulus of Nafion/PW-mGO and recast Nafion membranes was 243 and 159 MPa, respectively. On the other hand, the tensile strength of Nafion/PW-mGO, and recast Nafion membranes was 13 and 11 MPa, respectively. The composite membrane exhibited higher maximum stress at break and young modulus than recast Nafion membrane. This suggests that upon introducing PW-mGO nanohybrid filler to the Nafion ionomer improves the mechanical property of composite membrane when compared with pristine Nafion membrane.

Conclusions

We successfully incorporated functionalized reduced GO with phosphotungstic acid in a Nafion membrane, which services as water resource at relative low humidity. The PW-mGO

hybrid had strong electrostatic interaction with both the counter cations on mGO and phosphotungstic acid. Also, phosphotungstic acid possess high amount of water molecules with their acidic properties and water bound condition. Compared to Nafion-212 and Nafion/PW-mGO composite membranes, the Nafion/PW-mGO composite membranes exhibited remarkably better PEFC performance with operation under low RH.

Experimental Details

Preparation of graphene oxide

Graphene oxide (GO) was synthesized from graphite powder by a modified Hummer method.³⁸ One gram of graphite powder (Sigma Aldrich) was thoroughly ground with sodium chloride (50 g, Daejung, Seoul, Korea) and the mixture washed with de-ionized (DI) water and ethanol 5~10 times to remove sodium chloride. After drying, 4 mL of H₂SO₄ (Sigma Aldrich, 99%) was added and mixed with 0.84 g of K₂S₂O₈ (Kanto, Japan) and P₂O₅ (Kanto, Japan) at 80 °C (375 rpm) for 4.5 h. After the mixture cooled for 10~20 minutes, 167 mL of DI water was added and the mixture was stirred overnight at room temperature. The mixture was then filtered and washed using DI water and ethanol, and subsequently dried for 1 h. The collected powder was added to 40 mL of H₂SO₄ with 5 g of KMnO₄ (Aldrich) in a two-neck flask placed in an ice bath and stirred slowly until the contents were completely dissolved. Then, 84 mL of DI water was added into the mixture, which was stirred for 2 h at 35 °C. Finally, more DI water (167 mL) was added along with 10 mL of H₂O₂ (Samchun, Korea) and the reaction was terminated via stirring for 30 minutes in an ice bath. The resulting mixture was centrifuged until reaching pH 7, and then a brown powder was collected after drying in a vacuum oven.

Preparation of reduced graphene oxide (rGO)

Graphene oxide (GO, 1 g) was dispersed in 250 mL of DI water for 30 minutes. Five mL of hydrazine hydrate (Aldrich) was added into the mixture, which was then stirred for 4 h at

100 °C under a nitrogen atmosphere. Finally, the resulting mixture was filtered and washed until reaching pH 7, and then dried at 40 °C for 24 h in a vacuum oven.

Preparation of modified graphene oxide (mGO)

Reduced graphene oxide (rGO, 0.1g) was dispersed in 50 mL toluene (Aldrich) for 30 min. 3-aminopropyl-triethoxysilane (APTES, 0.1 g) was added into the rGO dispersion and stirred the contents for another 3 h at 30 °C and for 3 h at 100 °C under nitrogen atmosphere for condensation reaction. Finally, the resulting mixture was filtered and dried at 40 °C for 24 h in a vacuum oven after washing residual APTES by toluene.

Preparation of PW-mGO hybrid material

Modified graphene oxide (mGO, 0.1 g) was dispersed in 20 mL water and sonicated in DI water for 30 min by using an ultrasonicator. Aqueous solutions of 20 mgmL⁻¹ of phosphotungstic acid (H₃PW₁₂O₄₀, PW) n-hydrate (Kanto, Tokyo, Japan) was added to the mGO dispersion and stirred for 24 h. Finally, the resulting contents were filtered and washed three times with DI water to remove residual physically absorbed PW on the mGO, and dried at 60 °C for overnight in a vacuum oven.

Preparation of Nafion/ PW-mGO composite membrane

PW-mGO or mGO was impregnated in Nafion ionomer with a mass ratio of 1% and the resultant admixtures were ultra-sonicated for 30 min followed by mechanical stirring for 12 h. The composite membranes were prepared by casting these solutions on a glass petri dish and allowed to dry overnight at 80 °C using vacuum oven. The formed composite membranes were peeled off and further dried at 120 °C for 5 h. For comparison, Nafion ionomer was cast in a similar manner without any filler materials. The dry membrane thicknesses of all the composite membranes were measured at 5 random points over the surface using a digital micrometer and the average thickness was found to be ~ 40 μm. Finally, the membranes were

pre-treated by boiling in 5% H₂O₂, H₂O, 0.5 M H₂SO₄ and H₂O in sequence for 1 h in each case.

† Electronic Supplementary Information (ESI) available: Experimental and additional characterization data including TGA, CV stability and fuel cell performance under 100%RH at 100 °C.

Acknowledgments

This work was supported by the DGIST R&D Program (15-BD-01) of the Ministry of Education, Science and Technology of Korea. Part of this work also supported by the Basic Science Research Program through the National Research Foundation of Korea (NRF) funded by the Ministry of Education, Science, and Technology (2014R1A1A2057056).

References

- (1) B. C. H. Steele and A. Heinzl, *Nature*, 2001, **414**, 345-352.
- (2) S. M. Haile, D. A. Boysen, C. R. I. Chisholm, R. B. Merle, *Nature*, 2001, **410**, 910-913.
- (3) Z. Zuo, Y. Fu and A. Manthiram, *Polymers*, 2012, **4**, 1627-1644.
- (4) E. Aleksandrova, R. Hiesgen, A. Friedrich and E. Roduner, *Phys. Chem. Chem. Phys.*, 2007, **9**, 2735-2743.
- (5) K. A. Mauritz and R. B. Moore, *Chem. Rev.*, 2004, **104**, 4535-4586.
- (6) K.-D. Kreuer, S. J. Paddison, E. Spohr and M. Schuster, *Chem. Rev.*, 2004, **104**, 4637-4678.
- (7) K. Schmidt-Rohr and Q. Chen, *Nat. Mater.*, 2007, **7**, 75-83.
- (8) C. Wang, V. Krishnan, D. Wu, R. Bledsoe, S. J. Paddison and G. Duscher, *J. Mater. Chem. A*, 2013, **6**, 938-944.

- (9) H. B. Aiyappa, S. Saha, P. Wadge, R. Benerjee and S. Kurungot, *Chem. Sci.*, 2015, **6**, 603-607.
- (10) X. Liang, F. Zhang, W. Feng, X. Zou, C. Zhao, H. Na, C. Liu, F. Sun and G. Zhu, *Chem. Sci.*, 2013, **4**, 983-992.
- (11) M. K. Mistry, N. R. Choudhury, N. K. Dutta, R. Knott, Z. Shi and S. Holdcroft, *Chem. Mater.*, 2008, **20**, 6857-6870.
- (12) H. L. Tang and M. Pan, *J. Phys. Chem. C*, 2008, **112**, 11556-115568.
- (13) A. K. Sahu, S. D. Bhat, S. Pitchumani, P. Sridhar, V. Vimalan, C. George, N. Chandrakumar and A. K. Shukla, *J. Membr. Sci.*, 2009, **345**, 305-314.
- (14) V. Baglio, A. S. Aricò, A. D. Blasi, V. Antonucci, P. L. Antonucci, S. Licoccia, E. Traversac and F. Serraino Fiory, *Electrochim. Acta*, 2005, **50**, 1241-1246.
- (15) K. Ketpang, K. Lee and S. Shanmugam, *Appl. Mater. Interfaces*, 2014, **6**, 16734-16744.
- (16) T. Kim, Y.-W. Choi, C.-S. Kim, T.-H. Yang and M.-N. Kim, *J. Mater. Chem.*, 2011, **21**, 7612-7621.
- (17) W. Zhang, M. K. S. Li, P.-L. Yue and P. Gao, *Langmuir*, 2008, **24**, 2663-2670.
- (18) Y. Kim, S. Shanmugam, *ACS Appl. Mater. Inter.*, 2013, **5**, 12197-12204.
- (19) E. A. Ukshe, L. S. Leoniva and A. I. Korostelua, *Solid State Ionics*, 1989, **36**, 219-223.
- (20) S. Shanmugam, B. Viswanathan and T. K. Varadarajan, *J. Membr. Sci.*, 2006, **275**, 105-109.
- (21) W. Liu, W. Mu, M. Liu, X. Zhang, H. Cai and U. Deng, *Nat. Commun.*, 2014, **5**:3208, doi:10.1038/ncomms4208.
- (22) V. Ramani, H. R. Kunz and J. M. Fenton, *J. Mem. Sci.*, 2004, **232**, 31-44.
- (23) B. Stuart, *Infrared Spectroscopy: Fundamentals and Applications*. 2004.
- (24) R. Kumar, C. Xu and K. Scott, *RSC Adv.*, 2012, **2**, 8777-8782.
- (25) R. Kannan, B. A. Kakade and V. K. Pillai, *Angew. Chem. In. Ed.*, 2008, **47**, 2653-2656.

- (26) A. Enotiadis, K. Angjeli, N. Baldino, I. Nicotera and D. Gournis, *Small*, 2012, **8**, 3338-3349.
- (27) H. Zarrin, D. Higgins, Y. Jun, Z. Chen and M. Fowler, *J. Phys. Chem. C*, 2011, **115**, 20774-20781.
- (28) R. R. Abbaraju, N. Dasgupta and, A. V. Virkar, *J. Electrochem. Soc.*, 2008, **155**, B1307-B1313.
- (29) A. K. Sahu, S. Pitchumani, P. Sridhar and A. K. Shukla, *Fuel Cells*, 2009, **9**, 139-147.
- (30) A. D' Epifanio, M. A. Navarra, F. C. Weise, B. Mecheri, J. Farrington, S. Licoccia and S. Greenbaum, *Chem. Mater.*, 2010, **22**, 813-821.
- (31) Z.-G. Shao, P. Joghee and I-M. Hsing, *J Membr. Sci.*, 2004, **229**, 43-51.
- (32) M. Amirinejad, S. S. Madaeni, E. Rafiee and S. Amirinejad, *J. Membr. Sci.*, 2011, **377**, 8 9-98.
- (33) V. Ramani, H. R. Kunz and J. M. Fenton, *Electrochim Acta*, 2005, **50**, 1181-1187.
- (34) D. C. Lee, H. N. Yang, S. H. Park and W. J. Kim, *J. Membr. Sci.*, 2014, **452**, 20-28.
- (35) R. Kumar, and K. Scott, *Chem. Commun.*, 2012, **48**, 5584-5586.
- (36) J. Zeng and S. P. Jiang, *J. Phys. Chem. C*, 2011, **115**, 11854-11863.
- (37) K. -D. Kreuer, *Chem. Mater.*, 1996, **8**, 610-641.
- (38) W. S. Hummers and R. E. Offeman, *J. Am. Chem. Soc.*, 1958, **80**, 1339-1339.

Table 1. The electrochemical properties of PW-mGO and PW in 1 M H₂SO₄ at a scan rate of 25 mVs⁻¹.

Electrodes	E _{1ap} (mV)	E _{1cp} (mV)	ΔE ₁ (mV)	E _{3ap} (mV)	E _{3cp} (mV)	ΔE ₂ (mV)	E _{3ap} (mV)	E _{3cp} (mV)	ΔE ₃ (mV)
Pure PW	-8	-59	51	-272	-309	37	-611	-649	38
PW-mGO	-86	-140	54	-350	-370	20	-632	-638	6
Peak shift	78	81		78	61		21	11	

E_{1ap} – First anodic peak potential, E_{1cp} – First cathodic peak potential, ΔE – Peak separation

Table 2. The summary of fuel cell performance and membrane resistance of pristine and composite Nafion membranes operated under different temperatures and relative humidities

Membranes	80 °C, 100% RH			80 °C, 20% RH			100 °C, 100% RH		
	PD at 0.6 V	MR at 0.6 V	MPD	PD at 0.6 V	MR at 0.6 V	MPD	PD at 0.6 V	MR at 0.6 V	MPD
Recast Nafion	526	0.13	599	80	0.12	209	453	0.16	490
Nafion-212	556	0.14	598	90	0.10	210	462	0.18	500
Nafion/mGO	516	0.15	537	170	0.01	488	453	0.11	466
Nafion/mGO-PW	782	0.09	827	173	0.01	841	596	0.08	616

PD – Power density (mW cm^{-2}); MR – Membrane resistance (Ohm cm^{-2});

MPD – Maximum power density (mW cm^{-2})

Table 3. Comparison of fuel cell performance of various composite membranes under low RH.

Membranes	Max. power density/mW cm ⁻²	Conditions/ %RH, T °C	Reference
NRE-212	210		
Recast Nafion	208	20, 80	This study
Nafion/mGO	488		
Nafion/PW-mGO	841		
Nafion/TiO ₂ nanoparticles	327	25, 80	28
Nafion/TiO ₂ nanotube	641	18, 80	15
Nafion/MZP	350	18, 70	29
Nafion/S-ZrO ₂	600	30, 70	30
Nafion/SiO ₂	128	70, 110	31
Nafion/SiO ₂ -PWA	216	70, 110	31
Nafion/CsPMo	420	35, 80	32
Nafion/CsPW	350	35, 80	32
Nafion/modified PTA	210	35, 120	33
Nafion/GO	600	40, 80	34
Nafion/F-GO	150	25, 120	26
Nafion/Graphite oxide	212	25, 100	23
Sulfonated GO paper	100	25, 40	35

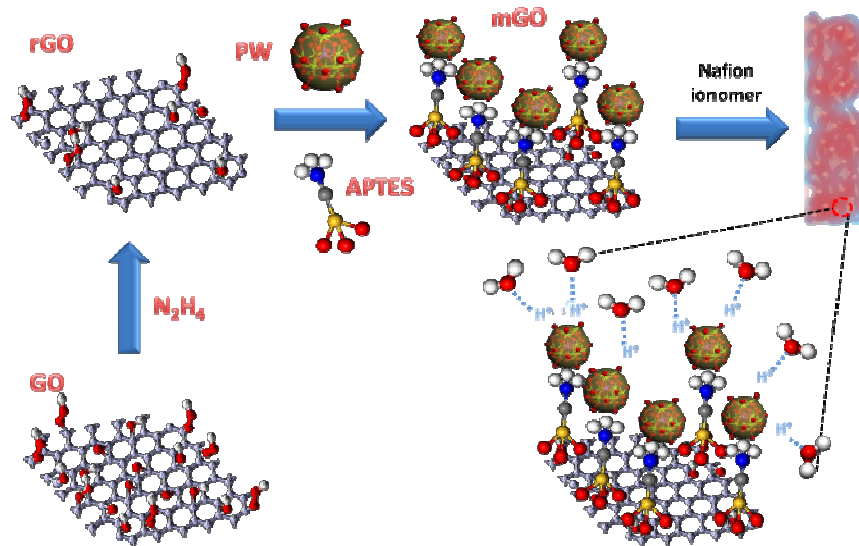


Fig. 1 Schematic representation of fabrication of phosphotungstic acid modified reduced graphene oxide-Nafion composite membrane.

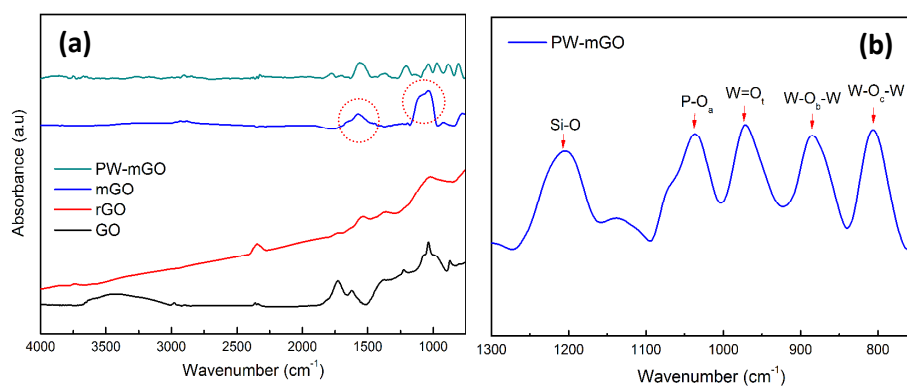


Fig. 2 (a) FT-IR spectra of GO, rGO, mGO, PW-mGO, the red circle marked are -NH_2 , and Si-O-Si bond, (b) metal-oxide stretching peak information of PW-mGO.

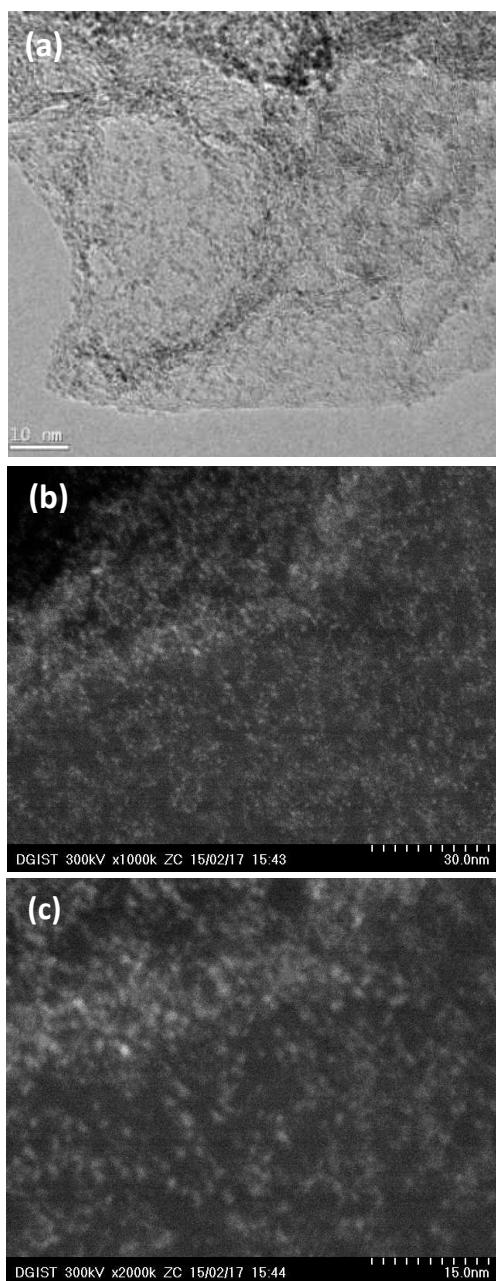


Fig. 3 (a) TEM and (b, c) STEM-HAADF images of PW-mGO hybrid. Bright spots represent PW clusters are well dispersed on graphene oxide surface.

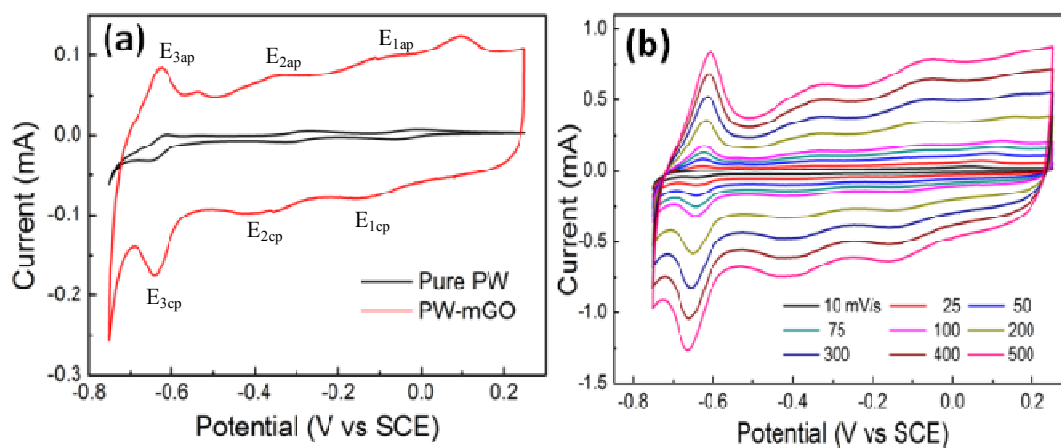


Fig. 4 (a) The comparison of CV of pure PW and PW-mGO at 25 mVs⁻¹ scan rate in 1 M H₂SO₄ electrolyte, (b) The effect scan rate of PW-mGO hybrid electrode.

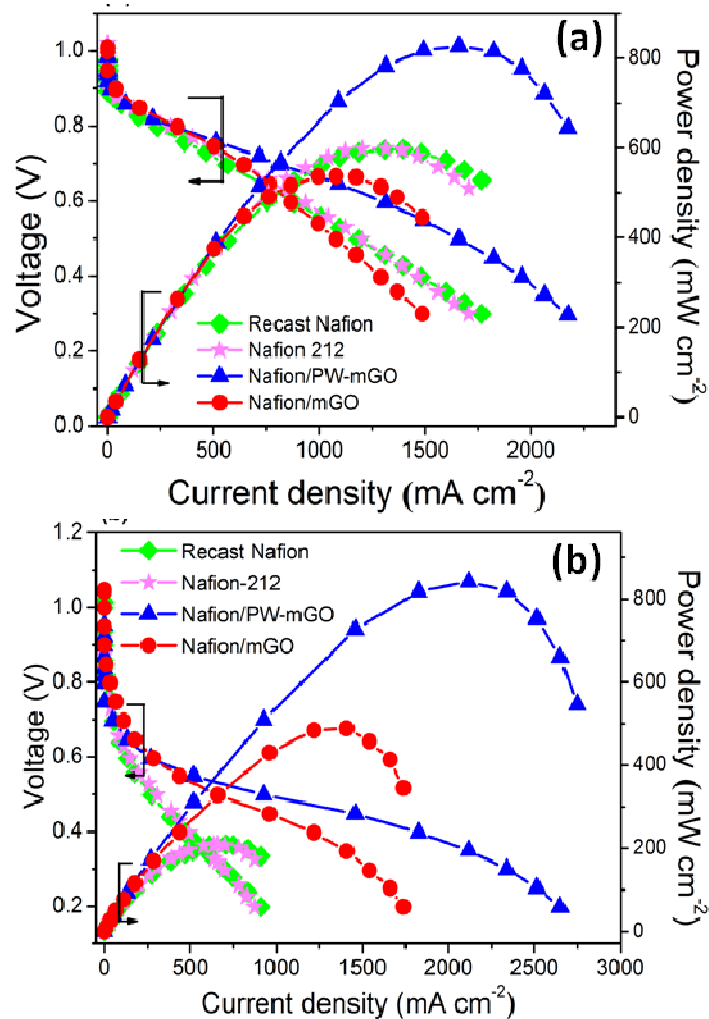


Fig. 5. Polarization and power density plots of (a) Nafion-212, recast Nafion, Nafion/mGO and Nafion/PW-mGO under 100%RH at 80 °C (b) operated under 20%RH at 80 °C. One weight percent filler content was used in composite membranes, catalyst loading in anode and cathode kept 0.5 mg/cm^2 .

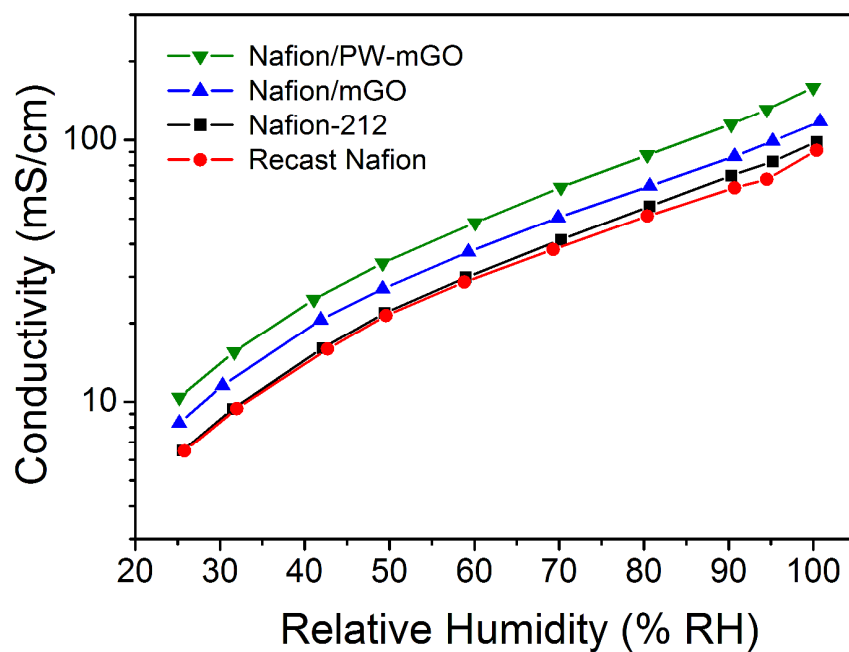


Fig. 6. Proton conductivity of Nafion-212, Nafion/mGO, and Nafion/PW-mGO composite membranes measured under different relative humidity at 80 °C

Table of Contents

Phosphotungstic acid coupled GO-Nafion membrane showed an enhanced fuel cell power density at 80°C under 20% RH, compared with Nafion-212.

